

BORROWING FROM ANYTHING: A GENERALIZABLE FRAMEWORK FOR REFERENCE-GUIDED INSTANCE EDITING

Shengxiao Zhou^{1,4} Chenghua Li^{2,*} Jianhao Huang^{1,3,4} Qinghao Hu^{3,4} Yifan Zhang^{3,4}

¹ University of Chinese Academy of Sciences, China

² Nanjing Forestry University, Nanjing, China

³ Institute of Automation, Chinese Academy of Sciences, Beijing, China

⁴ Nanjing Artificial Intelligence Research of IA, Nanjing, China

ABSTRACT

Reference-guided instance editing is fundamentally limited by semantic entanglement, where a reference’s intrinsic appearance is intertwined with its extrinsic attributes. The key challenge lies in disentangling what information should be borrowed from the reference, and determining how to apply it appropriately to the target. To tackle this challenge, we propose GENIE, a **GEN**eralizable **Instance Editing** framework capable of achieving explicit disentanglement. GENIE first corrects spatial misalignments with a Spatial Alignment Module (SAM). Then, an Adaptive Residual Scaling Module (ARSM) learns what to borrow by amplifying salient intrinsic cues while suppressing extrinsic attributes, while a Progressive Attention Fusion (PAF) mechanism learns how to render this appearance onto the target, preserving its structure. Extensive experiments on the challenging AnyInsertion dataset demonstrate that GENIE achieves state-of-the-art fidelity and robustness, setting a new standard for disentanglement-based instance editing. Code available at: <https://github.com/Xiao0219/GENIE.git>

Index Terms— Reference-Guided Image Editing, Progressive Attention Fusion, Adaptive Residual Scaling Module

1. INTRODUCTION

The essence of reference-guided instance editing [1–8] is to transfer the intrinsic appearance of a reference object, such as texture and patterns, to achieve fine-grained manipulation of a target. However, this task faces a fundamental challenge: semantic entanglement. In the reference features, the desired intrinsic appearance is inherently mixed with its incidental extrinsic attributes, such as pose, scale, and illumination. Lacking a dedicated mechanism to separate these, prior methods [2, 5] often suffer from artifacts like appearance leakage or identity distortion. We contend that effective feature disentanglement is the key to unlocking high-fidelity and controllable editing.

To this end, we propose GENIE, a framework designed to tackle entanglement through spatial alignment and appearance purification. The process begins with a Spatial Alignment Module (SAM), which canonicalizes reference features by correcting pose and scale variations in the latent space. After alignment, disentanglement is achieved by two synergistic modules that learn what and how to borrow: the Adaptive Residual Scaling Module (ARSM) purifies appearance cues by adaptively amplifying salient intrinsic appearance while suppressing irrelevant extrinsic attributes, and the Progressive Attention Fusion (PAF) mechanism then renders this purified appearance onto the target’s geometry, preserving identity. Our main contributions are:

- We identify semantic entanglement as the core bottleneck and propose GENIE, a new framework that explicitly addresses it.
- We design a novel architecture with three synergistic modules that disentangles intrinsic appearance and extrinsic attributes in a structured manner.
- We achieve state-of-the-art performance on the challenging AnyInsertion [3] dataset, establishing a strong baseline for disentanglement-based editing.

2. RELATED WORK

Recent years have witnessed rapid progress in reference-guided image editing using diffusion models. Early methods such as Paint-by-Example [2] and MimicBrush [1] explored example-based or zero-shot semantic editing, enabling object replacement, style imitation, and seamless blending. For object insertion and composition, recent works have made key advances: AnyDoor [5] tackled zero-shot object transfer; ObjectStitch [9] enhanced geometric and lighting consistency via self-supervision; and InsertAnything [3], leveraging diffusion Transformers, achieved context-aware insertion. In image completion, CompleteMe [10] retained fine-grained details via a dual U-Net with regional attention, while FreeEdit [11] achieved mask-free, multi-modal reference-guided editing. In virtual try-on, IMAGDressing [12], IDM-VTON [13] and OOTDiffusion [4] emphasized clothing semantic modeling and detail consistency, highlighting the potential of diffusion models in fashion applications. Additionally, EfficientMT [14] extended reference-guided editing to videos, supporting temporal adaptation and motion transfer.

Overall, these methods excel in zero-shot editing and detail preservation, but struggle to disentangle semantic features from the reference. Relatively, our method explicitly disentangles these features to achieve high-fidelity instance editing.

3. METHOD

3.1. Overall Framework

As illustrated in Fig. 1, we present GENIE, a dual U-Net latent diffusion model [15], comprising a reference branch for appearance disentanglement and a target branch for denoising synthesis. It takes a reference image $I_{ref} \in \mathbb{R}^{H \times W \times 3}$, a target image $I_{tar} \in \mathbb{R}^{H \times W \times 3}$, and a binary mask $M \in \{0, 1\}^{H \times W}$ as input, aiming to extract appearance features from the reference to guide the editing process.

The reference branch aims to disentangle the reference image I_{ref} . Specifically, I_{ref} is processed by a VAE encoder [16] and Spatial Alignment Module to obtain an aligned feature F_r , which is then fed into the reference U-Net (U_{ref}). Within the mid-block and

*Corresponding Author

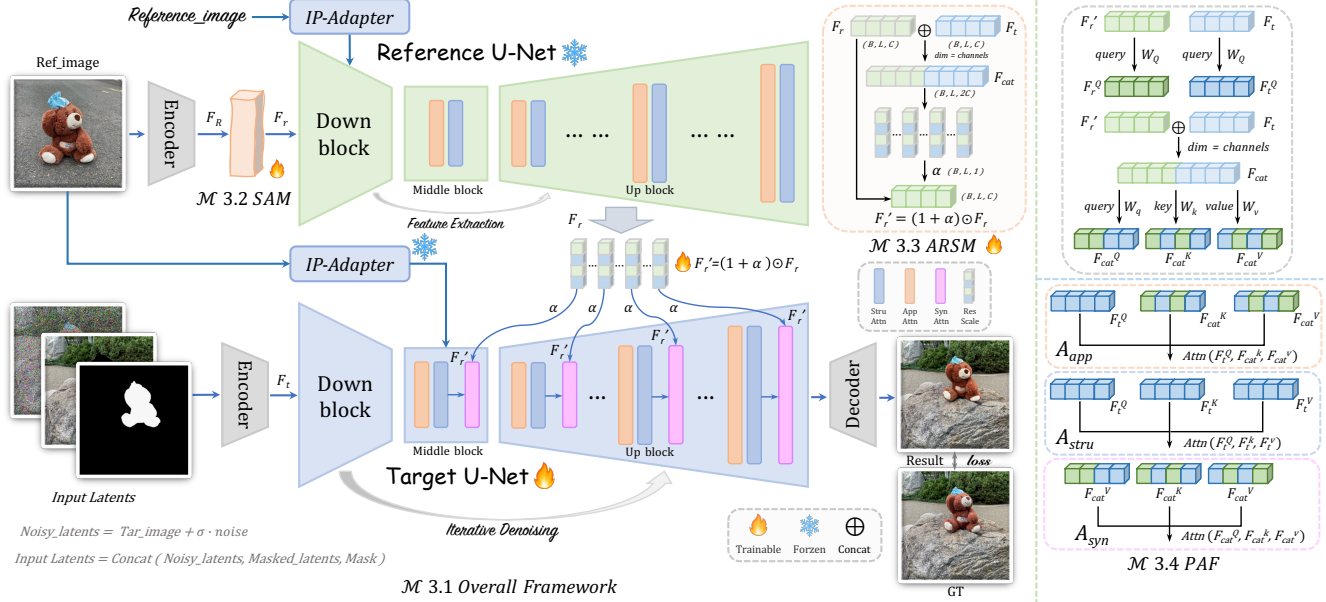


Fig. 1: Overview of the GENIE model framework.

up-sampling blocks of U_{ref} , the Adaptive Residual Scaling Module computes a target-aware scale map to purify features by amplifying salient intrinsic appearance cues while simultaneously suppressing confounding extrinsic attributes. The resulting disentangled feature, F_r' , is subsequently injected into the target branch.

The target branch, implemented as a U-Net (U_{tar}), is responsible for the iterative denoising process. At each timestep t , its input F_t is formed by the channel-wise concatenation of the noisy latent z_t , the mask representation $\phi(M)$, and the latent of the unedited region z_{masked} from $I_{tar} \odot (1 - M)$. The semantic information is injected into the U_{tar} using IP-Adapter [17], after which the disentangled reference feature F_r' is fused into U_{tar} via Progressive Attention Fusion mechanism. The entire framework is optimized end-to-end by minimizing the standard noise prediction objective:

$$\mathcal{L} = \mathbb{E}_{z_0, \epsilon \sim \mathcal{N}(0,1), F_t, F_r', t} \|\epsilon_\theta(z_t, F_t, F_r', t) - \epsilon\|^2, \quad (1)$$

where ϵ_θ represents our dual U-Net model, conditioned on both the target conditions F_t and the purified reference features F_r' .

3.2. Spatial Alignment Module (SAM)

To address the interference from extrinsic attributes such as an object's pose and scale, we propose the Spatial Alignment Module, which learns to produce a spatially normalized feature map F_r from the input feature F_R . This is accomplished by first employing a localization network, f_{loc} , to predict a 2D affine transformation tailored to the input, and then applying this transformation to warp the feature map [18]. This differentiable process is formulated as:

$$F_r = \mathcal{T}_{f_{loc}(F_R)}(F_R). \quad (2)$$

3.3. Adaptive Residual Scaling Module (ARSM)

In reference-based image editing, the core challenge lies in disentangling the entangled intrinsic appearance and extrinsic attributes within reference features, which is the root cause of artifacts such as identity leakage and pose residue.

To this end, we propose the Adaptive Residual Scaling Module (ARSM), which learns a target-aware spatial scaling map α to achieve precise adaptive modulation [14, 19]. Specifically, the reference feature F_r and the target feature F_t are concatenated along the channel dimension and input into a lightweight convolutional network, f_{scale} , to predict the scaling map:

$$\alpha = \tanh(f_{scale}(F_r \oplus F_t)). \quad (3)$$

The tanh function constrains α to $(-1, 1)$, making it a bidirectional modulation signal: positive values enhance the intrinsic appearance, while negative values suppress the extrinsic attributes. Finally, the disentangled feature F_r' is generated through a residual [20] scaling operation, $F_r' = (1 + \alpha) \odot F_r$. This design transforms the learned modulation signal α into a scaling factor within the $(0, 2)$ range, enabling continuous control from suppression to enhancement, and ultimately generates a more purified and robust appearance representation to guide the subsequent generation.

3.4. Progressive Attention Fusion (PAF)

To precisely fuse the decoupled appearance features F_r' into the U-Net's feature map F_t while preserving structural integrity, we design the Progressive Attention Fusion mechanism. Our core idea is that an effective fusion should follow a progressive strategy: first stabilize the structure, then explore associations, and finally guide the rendering. As illustrated in Figure 1, the PAF is composed of Structural Attention, Synergistic Attention, and Appearance Attention, which work in concert to achieve a precise and robust feature fusion.

First, the Structural Attention exclusively focuses on the input structural features F_t . By capturing its spatial context, it refines and reinforces the geometric layout, yielding the output $A_{stru} = \text{Attn}(F_t^q, F_t^k, F_t^v)$, which provides a stable foundation for the subsequent fusion.

Second, the Synergistic Attention concatenates the structural features F_t and appearance features F_r' into a hybrid feature map

Table 1: Quantitative results on the AnyInsertion Dataset. Red and blue indicate the best and second-best, respectively.

Category	Method	PSNR \uparrow	SSIM \uparrow	LPIPS \downarrow	CLIP \uparrow	DINO \uparrow	DreamSim \downarrow	FID \downarrow
Object (512*512)	AnyDoor [5]	17.9390	0.7266	0.2183	84.31	83.96	0.2183	127.2127
	Paint-by-Example [2]	23.6882	0.8967	0.0996	90.94	89.38	0.1124	91.1069
	MimicBrush [1]	23.9651	0.8740	0.0925	93.40	93.48	0.0819	79.7223
	Insert Anything [3]	23.6183	0.8381	0.1083	94.13	95.18	0.0644	76.6867
	Average (Ours)	26.3391	0.9160	0.0673	94.28	94.55	0.0652	68.9357
Garment (512*512)	Paint-by-Example [2]	20.2064	0.8451	0.1334	87.47	83.35	0.1441	88.9629
	MimicBrush [1]	21.8371	0.8480	0.0962	94.05	92.32	0.0873	63.2055
	OOTDiffusion [4]	20.2171	0.8497	0.1117	91.00	89.38	0.0989	71.2808
	Insert Anything [3]	21.0330	0.8173	0.1060	93.23	95.31	0.0638	53.9997
	Average (Ours)	23.8932	0.8740	0.0711	94.98	94.96	0.0573	40.7161
Person (512*512)	AnyDoor [5]	12.5243	0.5437	0.4385	68.02	65.65	0.3634	225.1038
	Paint-by-Example [2]	17.8149	0.7502	0.2265	84.89	80.38	0.1975	186.4751
	MimicBrush [1]	24.0970	0.8377	0.0994	94.37	94.18	0.0732	124.0520
	Insert Anything [3]	21.2598	0.7578	0.1588	92.71	93.32	0.0745	102.1670
	Average (Ours)	24.1848	0.8363	0.0973	94.79	94.22	0.0645	85.5789

Table 2: Ablation study of components (O=Object, G=Garment, P=Person, B=Baseline, S=SAM, F=PAF, A=ARSM). Best results are bold.

Method	PSNR \uparrow			SSIM \uparrow			LPIPS \downarrow			CLIP \uparrow			DINO \uparrow			DreamSim \downarrow			FID \downarrow		
	O	G	P	O	G	P	O	G	P	O	G	P	O	G	P	O	G	P	O	G	P
B	23.96	21.83	24.09	0.874	0.848	0.837	0.092	0.096	0.099	93.40	94.05	94.37	93.48	92.32	94.18	0.081	0.087	0.073	79.72	63.20	124.05
B+S	24.67	22.21	23.46	0.890	0.860	0.826	0.077	0.083	0.103	94.16	94.40	94.71	93.93	93.89	94.19	0.069	0.073	0.070	74.54	53.43	93.30
B+S+F	26.20	23.80	24.15	0.914	0.873	0.834	0.067	0.072	0.092	94.15	94.70	94.70	94.50	94.75	94.15	0.062	0.058	0.078	70.12	52.31	88.64
B+S+F+A	26.34	23.89	24.18	0.916	0.874	0.836	0.067	0.071	0.097	94.28	94.98	94.79	94.55	94.96	94.22	0.065	0.057	0.065	68.93	40.71	85.58

F_{cat} . It then performs self-attention within this shared space to explore the latent relationships between structure and appearance, creating a rich feature pool calculated as $A_{syn} = \text{Attn}(F_{cat}^q, F_{cat}^k, F_{cat}^v)$.

Finally, the Appearance Attention performs structure-guided rendering. It executes a cross-attention operation with the input structural feature F_t and the hybrid feature map F_{cat} , enabling the structure to actively query and fuse the required appearance textures for a precise rendering, formulated as $A_{app} = \text{Attn}(F_t^q, F_{cat}^k, F_{cat}^v)$.

The outputs of these three branches, A_{stru} , A_{syn} , and A_{app} , are subsequently integrated via a dynamic weighted fusion to produce the final feature, F_{out} :

$$F_{out} = \beta \cdot A_{stru} + \gamma \cdot A_{syn} + \lambda \cdot A_{app}, \quad (4)$$

where β , γ , and λ are learnable scalar weights. This design allows the PAF mechanism to adaptively balance these three strategies in an end-to-end manner, ensuring the precision, robustness, and structural consistency of the feature fusion.

4. EXPERIMENTS

4.1. Implementation Details

4.1.1. Hyperparameters

The model is trained for 10 epochs on the AnyInsertion [3] dataset, with all images resized to a resolution of 512×512 . We employ the Adam optimizer [21] with a learning rate of 1×10^{-5} . The training is conducted on 8 NVIDIA A100 GPUs, utilizing a batch size of 14 per GPU for an effective total batch size of 112.

4.1.2. Evaluation Metrics

We conduct a comprehensive evaluation of our method from three key perspectives: (1) Perceptual Quality, assessed by LPIPS [22], DreamSim [23], and FID [24]; (2) Appearance Consistency, measured through feature-space cosine similarity with DINO [25] and CLIP [26]; (3) Reconstruction Accuracy, quantified using PSNR [27] and SSIM [28].

4.2. Comparisons with Other Methods

We compare our method with several representative reference-based image editing baselines: AnyDoor [5], Paint-by-Example [2], MimicBrush [1], and InsertAnything [3]. For garment editing, we additionally include OOTDiffusion [4]. For fair comparisons, we provide adapted inputs, such as reference masks, to all baselines.

4.2.1. Quantitative Comparison

Table 1 presents quantitative comparisons on the AnyInsertion dataset (512×512), where our method delivers the best overall performance. Across the complex Object and Garment categories, our approach ranks first on most metrics spanning fidelity and semantics (PSNR, SSIM, LPIPS, CLIP, FID). In the Person category, it continues to lead on all metrics except SSIM, demonstrating robust generalization. Notably, our method achieves substantial improvements over the strongest baselines, boosting PSNR by 2 dB on Objects and Garments, while significantly lowering FID scores by 7.75 and 13.28, respectively. For Persons, it reduces FID by 16.59, validating its superior ability to harmonize reconstruction accuracy with semantic coherence.

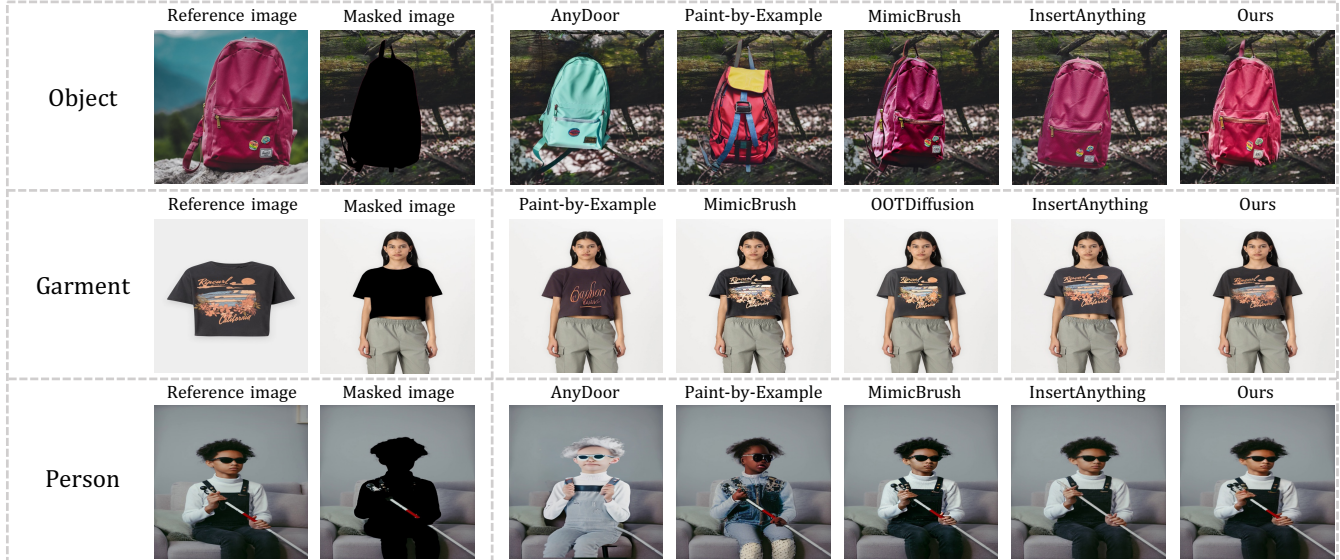


Fig. 2: Qualitative comparison of different methods.

Table 3: Training strategy ablation on AnyInsertion Dataset (O=Object, G=Garment, P=Person; R=Ref U-Net, T=Tar U-Net, I=IP-Adapter).

R T I	PSNR \uparrow			SSIM \uparrow			LPIPS \downarrow			CLIP \uparrow			DINO \uparrow			DreamSim \downarrow			FID \downarrow		
	O	G	P	O	G	P	O	G	P	O	G	P	O	G	P	O	G	P	O	G	P
✓ ✓ ✓	26.09	23.72	23.92	0.914	0.872	0.836	0.066	0.076	0.100	94.15	94.75	95.23	94.18	94.75	94.19	0.067	0.061	0.068	70.98	48.63	83.28
✓ ✓ X	25.82	23.03	24.15	0.913	0.870	0.827	0.069	0.079	0.101	94.31	94.51	95.12	94.22	93.66	94.38	0.069	0.065	0.065	71.25	47.13	80.91
✓ X X	25.50	22.80	23.50	0.910	0.868	0.829	0.071	0.082	0.103	94.00	94.20	94.70	94.10	93.50	94.02	0.070	0.066	0.066	72.50	49.50	86.20
✓ X ✓	25.70	22.95	23.65	0.912	0.869	0.834	0.070	0.080	0.101	94.05	94.35	94.85	94.20	93.60	94.10	0.069	0.065	0.066	71.90	48.90	85.72
X ✓ ✓	26.49	23.49	23.90	0.916	0.873	0.831	0.067	0.078	0.100	94.40	94.26	94.61	94.23	94.26	93.98	0.066	0.059	0.074	72.78	41.41	96.80
X ✓ X	26.34	23.89	24.18	0.916	0.874	0.836	0.067	0.071	0.097	94.28	94.98	94.79	94.55	94.96	94.22	0.065	0.057	0.065	68.94	40.72	85.58

4.2.2. Qualitative Comparison

As shown in Figure 2, our method demonstrates clear advantages across different categories. For the garment and person categories, the generated results preserve fine-grained details, accurately reconstructing clothing folds, fabric textures and subtle human structures. In the object category, our approach not only restores realistic details but also maintains natural texture and structural consistency. Importantly, the results are not achieved by simply pasting the reference image; instead, the inserted objects are seamlessly integrated into the background, producing visually coherent and harmonious outputs that highlight the model’s capability in both detail preservation and semantic fusion.

4.3. Ablation Study

4.3.1. Effectiveness Analysis of Key Components

Our ablation study in Table 2 cumulatively validates the effectiveness of each component. First, the Spatial Alignment Module (SAM) addresses geometric misalignment, drastically improving perceptual realism on the challenging Person dataset, as its FID score plummets from 124.05 to 93.30. Next, the Progressive Attention Fusion (PAF) is essential for high-fidelity reconstruction, evidenced by the significant leap in PSNR on the Garment dataset from 22.21 to 23.80. Finally, the Adaptive Residual Scaling Module (ARSM) showcases its feature disentanglement on the Object

dataset: while only improving PSNR by a marginal 0.14, its core impact is a dual enhancement of generative realism and semantic fidelity, reflected by the FID score decreasing from 70.12 to 68.93 and the CLIP score increasing from 94.15 to 94.28. These modules work in synergy to achieve the final, state-of-the-art performance.

4.3.2. Quantitative Analysis of Different Training Strategies

Our ablation study on training strategies, detailed in Table 3, reveals that the optimal approach is to freeze the Ref U-Net (R) and the IP-Adapter (I), while exclusively fine-tuning the Tar U-Net (T). This strategy preserves the powerful feature extraction capabilities of the pre-trained Ref U-Net and IP-Adapter modules, preventing knowledge degradation. The training is thereby concentrated on the Target U-Net, allowing it to specialize in effectively fusing and rendering these high-quality features, which leads to superior performance across the board.

5. CONCLUSION

We propose a framework to address the fundamental challenge of feature entanglement in reference-guided image editing. With modules for spatial alignment, appearance purification, and high-fidelity fusion, our method effectively disentangles reference information. Extensive experiments demonstrate the superiority of our method, which achieves state-of-the-art results on the AnyInsertion dataset.

6. ACKNOWLEDGMENTS

This work was supported by the Natural Science Foundation of Jiangsu Province under Grant BK20243051.

7. REFERENCES

- [1] X. Chen, Y. Feng, M. Chen, Y. Wang, S. Zhang, Y. Liu, Y. Shen, and H. Zhao, “Zero-shot image editing with reference imitation,” *Advances in Neural Information Processing Systems*, vol. 37, pp. 84 010–84 032, 2024.
- [2] B. Yang, S. Gu, B. Zhang, T. Zhang, X. Chen, X. Sun, D. Chen, and F. Wen, “Paint by example: Exemplar-based image editing with diffusion models,” in *Proceedings of the IEEE/CVF conference on computer vision and pattern recognition*, 2023, pp. 18 381–18 391.
- [3] W. Song, H. Jiang, Z. Yang, R. Quan, and Y. Yang, “Insert anything: Image insertion via in-context editing in dit,” *arXiv preprint arXiv:2504.15009*, 2025.
- [4] Y. Xu, T. Gu, W. Chen, and C. Chen, “Ootdiffusion: Outfitting fusion based latent diffusion for controllable virtual try-on,” in *Proceedings of the AAAI Conference on Artificial Intelligence*, 2025.
- [5] X. Chen, L. Huang, Y. Liu, Y. Shen, D. Zhao, and H. Zhao, “Anydoor: Zero-shot object-level image customization,” in *Proceedings of the IEEE/CVF conference on computer vision and pattern recognition*, 2024, pp. 6593–6602.
- [6] X. Zhang, J. Guo, P. Yoo, Y. Matsuo, and Y. Iwasawa, “Paste, inpaint and harmonize via denoising: Subject-driven image editing with pre-trained diffusion model,” *arXiv preprint arXiv:2306.07596*, 2023.
- [7] F. Peng, J. Wu, Y. Li, T. Gao, D. Zhang, and H. Fu, “Muse: Multi-subject unified synthesis via explicit layout semantic expansion,” in *Proceedings of the IEEE/CVF International Conference on Computer Vision (ICCV)*, 2025.
- [8] E. Ci, S. Guan, Y. Ge, Y. Zhang, W. Li, Z. Zhang, J. Yang, and Y. Tai, “Describe, don’t dictate: Semantic image editing with natural language intent,” in *Proceedings of the IEEE/CVF International Conference on Computer Vision (ICCV)*, 2025.
- [9] Y. Song, Z. Zhang, Z. Lin, S. Cohen, B. Price, J. Zhang, S. Y. Kim, and D. Aliaga, “Objectstitch: Generative object compositing,” *arXiv preprint arXiv:2212.00932*, 2022.
- [10] Y.-J. Tsai, B. Price, Q. Liu, L. Figuerola, D. Pakhomov, Z. Ding, S. Cohen, and M.-H. Yang, “Completeme: Reference-based human image completion,” *arXiv preprint arXiv:2504.20042*, 2025.
- [11] R. He, K. Ma, L. Huang, S. Huang, J. Gao, X. Wei, J. Dai, J. Han, and S. Liu, “Freedit: Mask-free reference-based image editing with multi-modal instruction,” *arXiv preprint arXiv:2409.18071*, 2024.
- [12] F. Shen, X. Jiang, X. He, H. Ye, C. Wang, X. Du, Z. Li, and J. Tang, “Imagdressing-v1: Customizable virtual dressing,” in *Proceedings of the AAAI Conference on Artificial Intelligence*, 2025.
- [13] Y. Choi, S. Kwak, K. Lee, H. Choi, and J. Shin, “Improving diffusion models for authentic virtual try-on in the wild,” *arXiv preprint arXiv:2403.05139*, 2024.
- [14] Y. Cai, H. Han, Y. Wei, S. Shan, and X. Chen, “Efficientmt: Efficient temporal adaptation for motion transfer in text-to-video diffusion models,” *arXiv preprint arXiv:2503.19369*, 2025.
- [15] R. Rombach, A. Blattmann, D. Lorenz, P. Esser, and B. Ommer, “High-resolution image synthesis with latent diffusion models,” in *Proceedings of the IEEE/CVF conference on computer vision and pattern recognition*, 2022, pp. 10 684–10 695.
- [16] D. P. Kingma and M. Welling, “Auto-encoding variational bayes,” in *Proceedings of the 2nd International Conference on Learning Representations (ICLR)*, 2014.
- [17] H. Ye, J. Zhang, S. Liu, X. Han, and W. Yang, “Ip-adapter: Text compatible image prompt adapter for text-to-image diffusion models,” *arXiv preprint arxiv:2308.06721*, 2023.
- [18] M. Jaderberg, K. Simonyan, A. Zisserman, and K. Kavukcuoglu, “Spatial transformer networks,” in *Advances in Neural Information Processing Systems*, vol. 28, 2015, pp. 2017–2025.
- [19] X. Liu, Y. Wei, M. Liu, X. Lin, P. Ren, X. Xie, and W. Zuo, “Smartcontrol: Enhancing controlnet for handling rough visual conditions,” *arXiv preprint arXiv:2404.06451*, 2024.
- [20] K. He, X. Zhang, S. Ren, and J. Sun, “Deep residual learning for image recognition,” in *Proceedings of the IEEE Conference on Computer Vision and Pattern Recognition (CVPR)*, 2016, pp. 770–778.
- [21] D. P. Kingma and J. Ba, “Adam: A method for stochastic optimization,” *arXiv preprint arXiv:1412.6980*, 2017.
- [22] R. Zhang, P. Isola, A. A. Efros, E. Shechtman, and O. Wang, “The unreasonable effectiveness of deep features as a perceptual metric,” in *Proceedings of the IEEE Conference on Computer Vision and Pattern Recognition (CVPR)*, 2018.
- [23] S. Fu, N. Tamir, S. Sundaram, L. Chai, R. Zhang, T. Dekel, and P. Isola, “Dreamsim: Learning new dimensions of human visual similarity using synthetic data,” *arXiv preprint arXiv:2306.09344*, 2023.
- [24] M. Heusel, H. Ramsauer, T. Unterthiner, B. Nessler, and S. Hochreiter, “Gans trained by a two time-scale update rule converge to a local nash equilibrium,” in *Advances in Neural Information Processing Systems*, vol. 30, 2017.
- [25] M. Caron, H. Touvron, I. Misra, H. Jégou, J. Mairal, P. Bojanowski, and A. Joulin, “Emerging properties in self-supervised vision transformers,” in *Proceedings of the IEEE/CVF international conference on computer vision*, 2021, pp. 9650–9660.
- [26] A. Radford, J. W. Kim, C. Hallacy, A. Ramesh, G. Goh, S. Agarwal, G. Sastry, A. Askell, P. Mishkin, J. Clark *et al.*, “Learning transferable visual models from natural language supervision,” in *International conference on machine learning*. Pmlr, 2021, pp. 8748–8763.
- [27] A. Hore and D. Ziou, “Image quality metrics: Psnr vs. ssim,” in *2010 20th International Conference on Pattern Recognition (ICPR)*. IEEE, 2010, pp. 2366–2369.
- [28] Z. Wang, A. C. Bovik, H. R. Sheikh, and E. P. Simoncelli, “Image quality assessment: from error visibility to structural similarity,” *IEEE Transactions on Image Processing (TIP)*, vol. 13, no. 4, pp. 600–612, 2004.